Stress Driven Flow with a Sloping Bottom

Lecture 6 by Frédéric Laliberté

In the preceding chapter, we investigated an isolated Ekman boundary layer for a sloping bottom in a stratified, rotating fluid. In this chapter, we intend to reconnect both the surface, stress driven boundary layer with a gently sloping bottom boundary layer.

1 Upwelling

The most physically stable case is without doubt the one leading to upwelling, a displacement that does not lead to a local inversion in the stratification. Indeed, if a volume of fluid is pushed upward along a sloping bottom, the only result in a hydrostatic point of view is a local increase in stratification, which negatively feedbacks on the ability of this volume to continue to move upward. So, one can easily argue that such a water movement must be relatively slow and strongly stratified near the bottom boundary. A flow with both of these qualities, one can argue, can only have (and will probably have) limited turbulence. Assuming that it is the case, one can thus start with the hypothesis that the flow will be laminar and smooth everywhere, including close to the boundary. This is a very desirable simplification that makes the upwelling case more physically tractable and intuitive, a path we will pursue first.

Oceanographically speaking, the problem we want to model is the upwelling on the continental shelf due an along shore wind stress resulting in a surface mass divergence. However, for our treatment to remain valid we must be sufficiently far from the shore so that we do not have to worry about our laminar bottom boundary layer merging with the surface Ekman layer. The schematic of the problem can be found in fig. 1. In this figure, the surface boundary layer transport results in a Coriolis force balancing the along shore wind stress τ. Again, we will be working in a rotated coordinate system so that the bottom slope corresponds to $z = 0$, i.e. the z axis is not parallel to the gradient of the geopotential (the gravitational force) but is instead perpendicular to the bottom.

1.1 Boussinesq equations

In order to study this problem without being systematically confusing which coordinate system is used, we will carefully restate the dimensional incompressible Boussinesq equations. If we use the usual cartesian coordinates with the z-coordinate parallel to the gravity, we have (for a reference see, for example, Vallis (2006)):

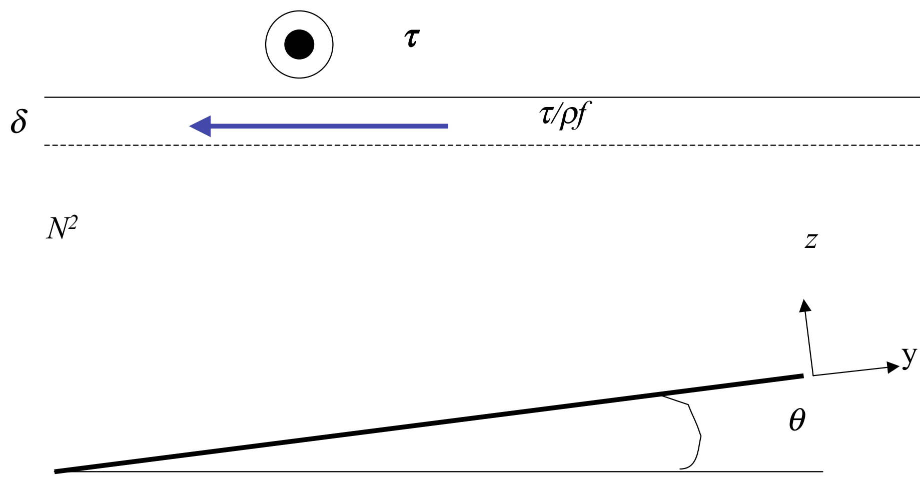

Figure 1: Idealized upwelling schematics on a sloping shelf away from shore. Notice the rotated coordinates

$$\partial_t \vec{u}' + \vec{u}' \cdot \nabla' \vec{u}' + f\hat{k}' \times \vec{u}' = -\frac{1}{\rho_0}\nabla' p + b\hat{k}' + \nabla' \cdot (\mathbf{A}'\nabla\vec{u}'), \tag{1}$$

$$\nabla' \cdot \vec{u}' = 0, \tag{2}$$

$$\partial_t b + \vec{u}' \cdot (\nabla' b + N^2 \hat{k}') = \nabla' \cdot (\boldsymbol{\kappa}' \nabla' b). \tag{3}$$

where $b = -g\tilde{\rho}/\rho_0$ and $N^2 = -g\partial_{z'}\bar{\rho}/\rho_0$, with $\rho = \rho_0 + \bar{\rho}'(z') + \tilde{\rho}'(\mathbf{x}', t)$.

1.2 Approximation for the sloping bottom

In the previous equations we have allowed the *eddy viscosity* $\mathbf{A}'$ and the *eddy diffusivity*, $\boldsymbol{\kappa}'$ to be anisotropic.

The next step is to apply these three approximations:

1. The flow is stationary, all the time derivatives vanish.
2. We linearize the flow about $\vec{u}' = 0$.
3. We rotate the axis in order to have the y axis parallel to the bottom slope, assuming the slope is extremely gentle. We will clarify later what it means for a slope to be small.

The resulting system of equations is

$$f\hat{n} \times \vec{u} = -\frac{1}{\rho_0}\nabla p + b\hat{n} + \nabla \cdot (\tilde{\mathbf{A}}\nabla\vec{u}), \tag{4}$$

$$\nabla \cdot \vec{u} = 0, \tag{5}$$

$$\vec{u} \cdot (\nabla b + N^2 \hat{n}) = \nabla \cdot (\tilde{\boldsymbol{\kappa}}\nabla b). \tag{6}$$

where all the quantities are now considered in the tilted frame and $\hat{n} = R\hat{k}'$, $\mathbf{A} = R\mathbf{A}'R^T$ and $\boldsymbol{\kappa} = R\boldsymbol{\kappa}'R^T$. These are simply the rotated values for the anisotropy vectors/tensors.

$$R = \begin{pmatrix} 1 & 0 & 0 \\ 0 & \cos\theta & \sin\theta \\ 0 & -\sin\theta & \cos\theta \end{pmatrix}, \quad \hat{n} = \begin{pmatrix} 0 \\ \sin\theta \\ \cos\theta \end{pmatrix}. \tag{7}$$

The anisotropic mixing coefficients will be assumed to be diagonal in the flow interior:

$$\mathbf{A}' = \begin{pmatrix} A_h & 0 & 0 \\ 0 & A_h & 0 \\ 0 & 0 & A_v \end{pmatrix}, \quad \boldsymbol{\kappa}' = \begin{pmatrix} \kappa_h & 0 & 0 \\ 0 & \kappa_h & 0 \\ 0 & 0 & \kappa_v \end{pmatrix}. \tag{8}$$

To obtain these tensors in the tilted frame we just have to apply the transformation, yielding:

$$\mathbf{A} = \mathbf{A}' + (A_v - A_h)\sin\theta\mathbf{O}, \quad \boldsymbol{\kappa} = \boldsymbol{\kappa}' + (\kappa_v - \kappa_h)\sin\theta\mathbf{O}. \tag{9}$$

where the matrix $\mathbf{O}$ is given by:

$$\mathbf{O} = \begin{pmatrix} 0 & 0 & 0 \\ 0 & \sin\theta & \cos\theta \\ 0 & \cos\theta & -\sin\theta \end{pmatrix} \tag{10}$$

We will further assume that the motion is *mostly independent of the x-x' coordinates* so that we can neglect all the x derivatives.

The final set of equations reduces to

$$-fv\cos\theta + fw\sin\theta = \nabla\cdot(\mathbf{A}\nabla u), \tag{11}$$

$$fu\cos\theta = -\frac{1}{\rho_0}\partial_y p + b\sin\theta + \nabla\cdot(\mathbf{A}\nabla v), \tag{12}$$

$$-fu\sin\theta = -\frac{1}{\rho_0}\partial_z p + b\cos\theta + \nabla\cdot(\mathbf{A}\nabla w), \tag{13}$$

$$\partial_y v + \partial_z w = 0, \tag{14}$$

$$v(N^2\sin\theta + \partial_y b) + w(N^2\cos\theta + \partial_z b) = \nabla\cdot(\boldsymbol{\kappa}\nabla b). \tag{15}$$

in the tilted frame.

1.3 Top boundary layer

In the gravitational frame, there will be a top boundary layer with pumping vertical velocity given by:

$$w' = w'_e = -\frac{1}{\rho_0 f}\partial_{y'}\tau \tag{16}$$

1.4 The interior solution

Vertical velocity Using the zonal momentum equation in the gravitational frame and non-dimensionalizing it with vertical scale D (of the ocean depth order), horizontal scale L, vertical velocity scale W and horizontal velocity scale U, we obtain,

$$-v_I' = \frac{A_v}{fD^2}(\partial_{z'}^2 u_I' + \frac{A_h}{A_v}\left(\frac{D}{L}\right)^2 \partial_{y'}^2 u_I'). \tag{17}$$

For geophysical flows, the aspect ratio $\frac{D}{L} \ll 1$ and we can expect, generally, that $A_v > A_h$ (intensified mixing in the vertical, a result of the possibility of isopycnals overturning). Labeling $E := \frac{A_v}{fD^2}$, we see that v_I' is $O(E)$.

With this result, we get from the continuity equation that $\partial_{z'} w'$ must be of $O(E \frac{D}{L} \frac{U}{W})$, implying that $w_I' \equiv w_e'$.

Buoyancy In order to find a suitable expression for the interior buoyancy, we can find a solution such that b is independent of z'. Neglecting v_I' comparatively to w_I', we obtain the following equation for b:

$$\kappa_h \partial_{y'}^2 b_I = w_I' N^2 \tag{18}$$

$$= -\frac{1}{\rho_0 f}\partial_{y'}\tau. \tag{19}$$

Assuming the wind stress disappears far from the shelf region, we obtain

$$\partial_{y'} b_I = -\frac{1}{\rho_0 f}\frac{N^2}{\kappa_h}\tau. \tag{20}$$

Zonal velocity Using the thermal wind balance, $f\partial_{z'} u_I' = -\partial_{y'} b_I$, we get

$$u_I' = \frac{N^2}{\kappa_h}\frac{\tau}{\rho_0 f^2} z' + u_{I0}'(y'). \tag{21}$$

Bottom buoyancy diffusive flux The flux perpendicular to the bottom boundary can be written as

$$\mathcal{F}_z = -\hat{k} \cdot (\boldsymbol{\kappa} \nabla b) = -\hat{k} \cdot (\tilde{\boldsymbol{\kappa}} \nabla' b). \tag{22}$$

What we want to do is to recast the insulated boundary condition, $b_{z'} = -N^2 \cos\theta$ as a boundary condition on the perpendicular flux, $\mathcal{F}_z$. This yields,

$$(\mathcal{F}_z)_{\text{ins}} = (\kappa_v \cos^2\theta - \kappa_h \sin^2\theta) N^2 \approx \kappa_v \cos\theta N^2. \tag{23}$$

to $O(\theta^2)$, where we have assumed that $\kappa_v \gg \kappa_h \cot^2(\theta)$. This is the condition of smallness required for θ.

Next, we want to find the contribution to the perpendicular flux by the interior solution:

$$(\mathcal{F}_z)_I = -\frac{\tau}{\rho_0 f}\sin\theta N^2. \tag{24}$$

The boundary condition should be

$$(\mathcal{F}_z)_{\text{tot}} = (\mathcal{F}_z)_{\text{ins}}. \tag{25}$$

which can only be satisfied, in general, with the boundary layer contribution.

1.5 Bottom boundary layer

As seen previously, when we had only a bottom layer, we can reduce the problem to

$$\partial_z^4 v_b + \frac{4}{l^4} v_b = 0, \tag{26}$$

where $l^{-4} = \frac{f^2}{4A_v^2}\left[1 + \frac{N^2 \sin^2\theta}{f^2 \kappa_v / A_v}\right]$.

Thus,

$$v_b = e^{-\frac{z}{l}}[A\cos(\frac{z}{l}) + B\sin(\frac{z}{l})], \tag{27}$$

$$u_b = \frac{f}{A_v}\frac{l^2}{2} e^{-\frac{z}{l}}[A\sin(\frac{z}{l}) - B\cos(\frac{z}{l})], \tag{28}$$

$$\partial_z b_b = -\frac{N^2}{2\kappa_v}\delta \sin\theta e^{-\frac{z}{l}}[A(\cos(\frac{z}{l}) - \sin(\frac{z}{l})) + B(\cos(\frac{z}{l}) + \sin(\frac{z}{l}))], \tag{29}$$

$$w_b = \frac{l}{2} e^{-\frac{z}{l}}[\partial_y A(\cos(\frac{z}{l}) - \sin(\frac{z}{l})) + \partial_y B(\cos(\frac{z}{l}) + \sin(\frac{z}{l})) + \sin(\frac{z}{l}))]. \tag{30}$$

1.6 Matching Solutions

In order to determine the integration constants, we need the interior solutions plus the boundary corrections to add up and satisfy the no-slip boundary condition. The interior fields at the bottom boundary yields

$$u_I = u_0'(y') = u_0', \tag{31}$$

$$v_I = \sin\theta w_I' = -\sin\theta \frac{1}{\rho_0 f}\partial_{y'}\tau', \tag{32}$$

$$w_I = \cos\theta w_I' = -\cos\theta \frac{1}{\rho_0 f}\partial_{y'}\tau', \tag{33}$$

$$\mathcal{F}_z = N^2(\kappa_v \cos\theta + \frac{\tau'}{\rho_0 f}\sin\theta). \tag{34}$$

It remains to match the solutions in order to satisfy the no-slip boundary condition:

$$u_{\text{tot}} = 0, \qquad u_0(y) - \frac{f}{A_v}\frac{l^2}{2}B = 0, \tag{35}$$

$$v_{\text{tot}} = 0, \qquad -\frac{1}{\rho_0 f}\partial_y \tau \sin\theta + A = 0, \tag{36}$$

$$w_{\text{tot}} = 0, \qquad -\frac{1}{\rho_0 f}\partial_y \tau + \frac{l}{2}(A + B) = 0, \tag{37}$$

$$(\mathcal{F}_z)_{\text{tot}} = (\mathcal{F}_z)_{\text{ins}}, \qquad \kappa_v \cos\theta N^2 + N^2 \frac{\tau}{\rho_0 f}\sin\theta - N^2 \frac{l}{2}\sin\theta(A + B) = 0. \tag{38}$$

Using the last equation we can recover

$$\frac{l}{2}(A + B) = \frac{\tau}{\rho_0 f} + \kappa_v \cot\theta, \tag{39}$$

the boundary layer mass flux.

The first term on the RHS corresponds to the surface offshore flux balancing the onshore bottom Ekman flux. The second term is the transport in bottom boundary layer induced by stratification and diffusion as in the previous solution.

Using the remaining equations, we obtain

$$A = \frac{1}{\rho_0 f}\partial_y \tau \sin\theta, \tag{40}$$

$$B = -A + \frac{2}{l}(\frac{\tau}{\rho_0 f} + \kappa_v \cot\theta), \tag{41}$$

$$u_0 = -\frac{f}{A_v}\frac{l^2}{2}B. \tag{42}$$

From now on, we will assume that $\frac{fl^2}{2A_v} = O(1)$.

The controlled interior along shore velocity is

$$u_I = \frac{fl^2}{2A_v}\left(\frac{\tau}{\rho_0 f}\left(\left[\frac{2N^2 A_v}{\kappa_h f^2 l^2}\right] z + \frac{2}{l}\right) - \frac{1}{\rho_0 f}\partial_y \tau \sin\theta + 2\kappa_v \cot\theta\right) \tag{43}$$

Of the three terms independent of z, the second one, the one of $O(\frac{1}{l})$, must be the dominant of these terms since l is a small length scale. Therefore, we have a good idea of how the boundary control affects the interior flow by comparing this term with the first term, the one dependent on z. Assuming z is of order D in the interior, we obtain the ratio:

$$r_{1/2} \approx \frac{N^2}{f^2}\frac{f}{\kappa_h}Dl \tag{44}$$

$$= \frac{N^2 D^2}{f^2 L^2}\frac{fL^2}{A_h(\kappa_h A_h)}\frac{l}{D} \tag{45}$$

$$= \frac{\sigma_h S}{E_h}E_v^{\frac{1}{2}} = \left[\frac{\sigma_h S}{E_v^{1/2}}\right]\left(\frac{E_v}{E_h}\right). \tag{46}$$

If $E_v/E_h = O(1)$ then if $\sigma_h S \gg E_v^{1/2}$, *the interior velocity is only marginally controlled by the boundary layer* and, hence, it must nearly satisfy the no slip boundary condition on $z = 0$ without the boundary layer.

The reader might remember that this has also been observed in the cylinder problem with strong stratification.

2 Turbulent bottom boundary layer

In figure 2 we show the schematics for an upwelling bottom boundary layer. During the process, denser water is brought up, under lighter water, hence enhancing the static stability. The situation for *downwelling* is fundamentally different in that it reduces the hydrostatic stability by forcing lighter fluid under a heavier fluid. This leads to local overturning and convective instability. We thus expect the presence of a thicker turbulent boundary layer as in the upwelling case. The schematics for the problem, usually referred to as the Chapman-LentzChapman and Lentz (1997) (CL) model, are shown in figure 3. In this figure, we have illustrated the physics of the boundary layer, where one expect the fluid to be well-mixed, with isopycnals normal to the bottom boundary.

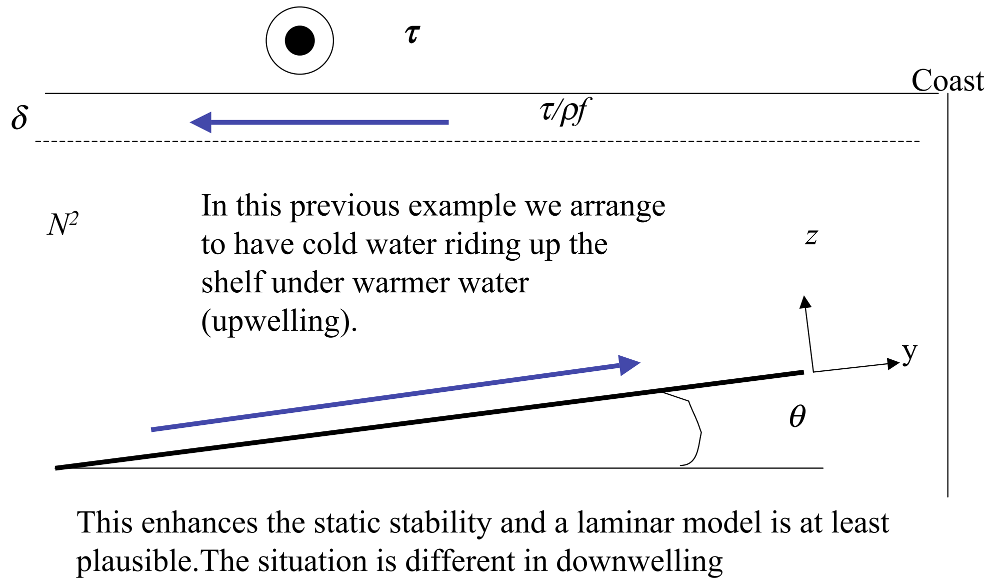

Figure 2: Idealized *upwelling* schematics on a sloping shelf away from shore. Notice the rotated coordinates

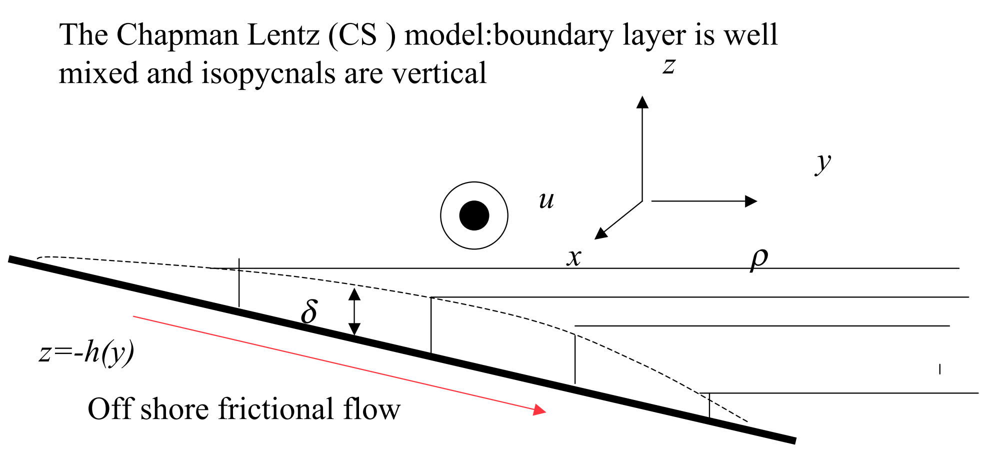

Figure 3: Schematics for the Chapman Lentz model for turbulent boundary layer

2.1 Model Equations

In this section, we return to the usual coordinates with unprimed variables corresponding to the frame where the z axis is parallel to the gravitational force. The model considers an hydrostatic flow and it neglects momentum advection. The equations read:

$$-fv = -\frac{1}{\rho_0}\partial_x p + \frac{1}{\rho_0}\partial_z \tau^x \tag{47}$$

$$fu = -\frac{1}{\rho_0}\partial_y p - g\rho \tag{48}$$

$$0 = -\partial_z p - g\rho \tag{49}$$

$$\partial_x u + \partial_y v + \partial_z w = 0 \tag{50}$$

$$u\partial_x \rho + v\partial_y \rho + w\partial_z \rho = \partial_y \left(\kappa_h \partial_y \rho\right) + \partial_z \left(\kappa_v \partial_z \rho\right). \tag{51}$$

where ρ is the perturbation density and B is the vertical turbulent density flux.

The interior flow is considered vertically uniform, therefore, all the partial derivatives in z vanish. All the turbulent effects including mixing, are assumed to be taking place in the bottom boundary layer that lies between $z = -h(y)$ and $z = -h(y) + \delta(x, y)$. Here, δ represent the boundary layer depth.

In the boundary layer, the mixing is assumed so intense that the fluid is vertically well-mixed, making the isopycnals perpendicular to the boundary. The boundary layer is also considered to be of sufficient extent that the intra boundary layer shears are not affected by the bottom friction. Instead, it is assumed that the horizontal variation in the density field are solely responsible for such shears.

2.1.1 Primary results

In their paper, Chapman & Lentz use slightly different equations and use them to derive a relation between p and δ, the thickness of the layer, where p decays like a one-dimensional diffusion equation, with x acting as time. This particular analysis is relevant for the problem of a coastal current, which definitely requires all three dimensions.

The current is thought to be narrow at the start and spread laterally due to friction, with the boundary layer thickening as the current flows downstream. One of the results of their model is that the boundary layer thickness evolves until the thermal winds brings u to zero, thus eliminating the bottom stresses. A schematic of this result is shown in figure 4. In figure 5, one will find one solution as computed by CL. It shows both the solution for a fixed stratification and for no stratification. The two leads to qualitatively very different results.

2.1.2 Further simplifications

Unlike in the previously mentioned reference, in order to carry tractable analysis further, we must make more simplifications. First, we assume that the forcing is independent of x, the along-shore coordinate. As a consequence, the boundary layer must transport mass offshore and the whole flow

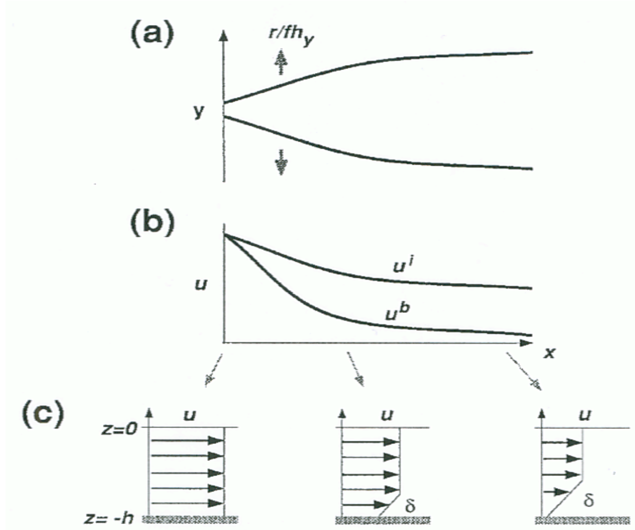

Figure 4: Schematic depicting the adjustment and evolution of a narrow inflow starting at $x = 0$. (a) Plan view of the current boundaries that initially spread, owing to bottom friction, at a rate set by $\frac{r}{fh_y}$, (b) Evolution of the interior velocity u^i and bottom velocity u^b with downstream distance. (c) Along-isobath velocity profiles at various stages downstream The bottom boundary layer grows, while the interior and bottom velocities both decrease, eventually reaching an equilibrium where the bottom velocity vanishes.

must be two-dimensional, resulting in the equations:

$$fu = -\frac{1}{\rho_0}\partial_y p, \tag{52}$$

$$-fv = \frac{1}{\rho_0}\partial_z \tau, \tag{53}$$

$$\frac{\rho}{\rho_0}g = -\frac{1}{\rho_0}\partial_z p, \tag{54}$$

$$\partial_y v + \partial_z w = 0, \tag{55}$$

$$v\partial_y \rho + w\partial_z \rho = \partial_y (\kappa_h \partial_y \rho) + \partial_z (\kappa_v \partial_z \rho). \tag{56}$$

2.1.3 Interior Flow

As before, the interior is to first order affected by the wind stress, τ^w, which produces an Ekman pumping

$$w = w_e = -\frac{1}{\rho_0 f}\partial_y \tau^w. \tag{57}$$

The bottom is assumed to lie at $z = -h(y) = -\alpha y + \delta$. with α a specified constant. At this boundary, we demand that the buoyancy flux normal to the bottom vanishes and all perturbations resulting from the boundary layer go to zero for large y. Moreover, we require that the density be continuous at the bottom since it is being mixed by the local turbulence.

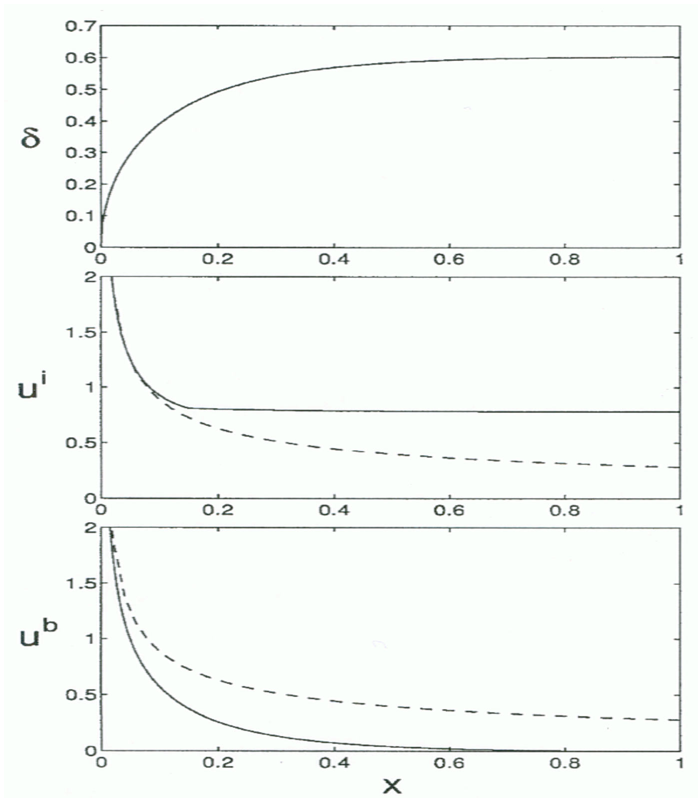

Figure 5: Maximum values of (upper) bottom boundary layer thickness, (middle) interior along-isobath velocity, and (lower) bottom velocity at each downstream (x) location. Dashed curves correspond to an unstratified flow.

Below the surface Ekman layer and above the bottom boundary layer, the turbulent stress in the fluid interior is zero, thus the interior velocity, v_I, must vanish as it is not affected by either of the boundary layers. This, as previously in this work, implies $w_I = w_e(y) = -\frac{1}{\rho_0 f}\partial_y \tau^w$.

Interior density equation With the results of the previous section, the density equation greatly simplifies in the interior:

$$w_e \partial_z \rho_I = \partial_y \left(\kappa_{h_I} \partial_y \rho_I\right) + \partial_z \left(\kappa_{v_I} \partial_z \rho_I\right). \tag{58}$$

The vertical density gradient is assumed to be constant, $\frac{g}{\rho_0}\partial_z \rho_I = -N^2$, which constrains the density to be

$$\frac{\rho_I}{\rho_0} = -z\frac{N^2}{g} - \int_y^\infty \frac{\tau^w}{\rho_0 f}\frac{N^2}{g\kappa_{h_I}} dy' + 1 \tag{59}$$

where we have chosen ρ_0 to be the surface density away from all perturbations.

Interior along shore velocity Using the thermal wind equation, we can recover the along shore interior velocity

$$\partial_z u_I = \frac{g}{f\rho_0}\partial_y \rho_I = \frac{\tau^w}{\rho_0 f^2}\frac{N^2}{\kappa_{h_I}}, \tag{60}$$

which yields

$$u_I = \frac{z}{\kappa_{h_I}}\frac{N^2}{f^2}\frac{\tau^w}{\rho_0} - \frac{1}{\rho_0 f}\partial_y p_s \tag{61}$$

where p_s, the barotropic pressure, is an unknown function.

2.1.4 Inside the bottom boundary layer

The model time scale is so large that the hydrostatically unstable region are assumed to overturn instantaneously, which is equivalent to assume a very intense mixing. This implies that $\rho_b(y) = \rho_I(y, z = -h(y) + \delta(y))$, i.e. the density in the boundary layer is independent of z and continuous with ρ_I at the separation interface, so density obeys.

$$\frac{\rho_b}{\rho_0} = (h-\delta)\frac{N^2}{g} - \int_y^\infty \frac{\tau^w}{\rho_0 f}\frac{N^2}{f\kappa_{h_I}} dy' + 1. \tag{62}$$

Pressure must be hydrostatic and continuous with the interior:

$$\frac{p_b}{\rho_0} = -(h-\delta)[z + \frac{h-\delta}{2}]N^2 + z\int_y^\infty \frac{\tau^w}{\rho_0 f}\frac{N^2}{f\kappa_{h_I}} dy' - gz + \frac{p_s}{\rho_0}. \tag{63}$$

Using the geostrophic balance for u, we can recover u_b,

$$u_b = \frac{N^2}{f}\partial_y((h-\delta)[z + \frac{h-\delta}{2}]) + z\frac{\tau^w}{\rho_0 f}\frac{N^2}{f\kappa_{h_I}} + \frac{1}{\rho_0 f}\partial_y p_s. \tag{64}$$

2.1.5 Finding the barotropic pressure

One unknown quantity that is left to be determined is the barotropic pressure p_s, used to define the along-shore velocities. In order to prescribe it, we use an Ekman bottom drag parameterization of the form

$$v_b\delta = \frac{ru_b(-h)}{f} \tag{65}$$

which enables us to write

$$-\frac{1}{\rho_0 f}\partial_y p_s = \frac{N^2}{f}\delta\partial_y(h-\delta) + h\frac{\tau^w}{\rho_0 f^2\kappa_{h_I}} + \frac{\tau^w}{\rho_0 r}. \tag{66}$$

in terms $\delta(y)$, a still undetermined quantity.

Boundary Layers velocities Having the barotropic pressure p_s, we can find the along-shore velocities,

$$u_b = \frac{N^2}{f}(z+h)\left[\partial_y(h-\delta) + \frac{\tau^w}{\rho_0 f\kappa_{h_I}}\right] + \frac{\tau^w}{\rho_0 r}, \tag{67}$$

$$u_I = \frac{N^2}{f}(z+h)\left[\frac{\tau^w}{\rho_0 f\kappa_{h_I}}\right] + \frac{N^2}{f}\delta\partial_y(h-\delta) + \frac{\tau^w}{\rho_0 r} \tag{68}$$

We observe that they are continuous at $z = -h+\delta$. We also observe that in the absence of stress the bottom velocity in the bottom boundary layer is zero as in MacCready and Rhines MacCready and Rhines (1993)

2.2 Budgets

In this section, we want to derive precise budgets for the different quantities of importance. In fig. 6 we show what the bottom boundary layer should look like.

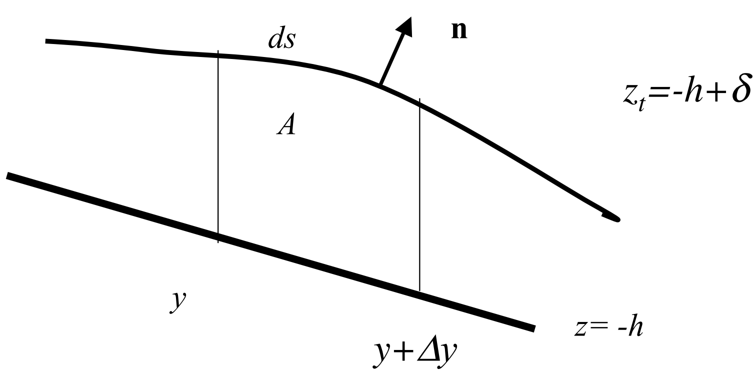

Figure 6: Schematics for the bottom boundary layer

2.2.1 Mass budget

In this problem, the Ekman flux from along-shore winds induce a shoreward mass flux that must be balanced by the bottom boundary transport. In order to make this intuitive idea more rigorous, we consider the vertical integral of the continuity equation, over the depth of the bottom boundary layer:

$$\int_{-h}^{-h+\delta} \partial_y v_b dz = 0. \tag{69}$$

where the part corresponding to the internal flow vanishes since the interior onshore velocity vanishes, $v_I = 0$.

If one integrates by parts,

$$0 = \partial_y \int_{-h}^{-h+\delta} v_b dz + [w_b(-h+\delta) - v_b(-h+\delta)\partial_y(-h+\delta)] + [w_b(-h) - v_b(-h)\partial_y(-h)], \tag{70}$$

$$= \partial_y(v_b\delta) + w_*, \tag{71}$$

where the first bracket corresponds to the flux across the boundary layer surface and the second bracket corresponds to the flux through the sea floor, a term that must vanish.

Since $v_I = 0$ and the problem has no x-dependence, the continuity equation implies that $w_* = w_e$. This mean that the mass budget is fully determined,

$$\partial_y(v_b\delta) - \frac{1}{\rho_0 f}\partial_y \tau^w = 0, \tag{72}$$

$$\Rightarrow \quad v_b\delta = \frac{\tau^w}{\rho_0 f}. \tag{73}$$

as expected.

2.2.2 Buoyancy budget

In this section we want to use the buoyancy equation, eq. 56,

$$v\partial_y\rho + w\partial_z\rho = \partial_y\left(\kappa_h\partial_y\rho\right) + \partial_z\left(\kappa_v\partial_z\rho\right). \tag{74}$$

First, we integrate it, making the vertical transport term disappear, leaving us with

$$v_b\delta\partial_y\rho_b dy = \mathcal{T}_b \cdot \hat{n} ds + \partial_y(\kappa_{h_b}\delta\partial_y\rho_b)dy, \tag{75}$$

where the first term on the rhs corresponds to the diffusive mass flux at the upper boundary of the bottom boundary layer. We have also used the fact that ρ_b is independent of z (the bottom layer is well-mixed).

Using a pill-box argument, one can show that the diffusive flux $\mathcal{T}_b$ must be continuous and, hence, it must be equal to the interior diffusive flux at the top of the bottom boundary layer $\mathcal{T}_b = \mathcal{T}_I$.

Thus, one can write

$$\mathcal{T}_b \cdot \hat{n}\frac{ds}{dy} = \mathcal{T}_I \cdot \hat{n}\frac{ds}{dy} = \kappa_{v_I}\partial_z\rho_I - \kappa_{h_I}\partial_y\rho_I\partial_y(-h+\delta). \tag{76}$$

Using the expressions for ρ_I and ρ_b in eq. 59 and in eq. 62, one can write an equation for δ:

$$\partial_y\left[\kappa_{h_b}\delta\partial_y(h-\delta) + \kappa_{h_b}\delta\frac{\tau^w}{\rho_0 f\kappa_{h_I}}\right] = \kappa_{v_I} + \frac{1}{\kappa_{h_I}}\left(\frac{\tau^w}{\rho_0 f}\right)^2 \tag{77}$$

2.2.3 Investigation of a special case

In this section, we want to investigate the solutions for a special case of bottom bathymetry and wind stress. As before, we use $h = -\alpha y$ and impose a stress of the form $\tau^w = \tau_0 e^{-a(y/L)}$.

The equation for δ becomes

$$\frac{d}{dy}\left[\delta\frac{d\delta}{dy} - (1 + Fe^{-ay})\delta\right] = -\Sigma_v - F^2\Sigma_h e^{-2ay} \tag{78}$$

where $F = \frac{\tau_0}{\alpha\rho_0 f\kappa_{h_I}}$, $\Sigma_v = \frac{\kappa_{v_I}}{\kappa_{h_b}\alpha^2}$ and $\Sigma_h = \frac{\kappa_{h_I}}{\kappa_{h_b}}$.

If one integrate this equation once,

$$\delta\partial_y\delta - (1 + Fe^{-ay})\delta = -\Sigma_v(y - y_0) - \frac{F^2}{2a}[e^{-2ay} - e^{-2ay_0}]\Sigma_h + C \tag{79}$$

where y_0 is the starting point of integration (we cannot deal with the singularity linked with the apex) and C is a constant of integration.

$$C = \left\{\delta\left[\frac{d\delta}{dy} - (1 + Fe^{-ay_0})\right]\right\}_{y=y_0} = \left\{\delta\left[-\frac{g}{\alpha N^2\rho_0}\partial_y\rho_b\right]\right\}_{y=y_0} < 0 \tag{80}$$

using the definition of ρ_b.

When δ goes to zero Knowing the internal velocity, given by eq. 68,

$$u_I = \frac{N^2}{f}(z + h)\left[\frac{\tau^w}{\rho_0 f\kappa_{h_I}}\right] + \frac{N^2}{f}\delta\partial_y(h - \delta) + \frac{\tau^w}{\rho_0 f} \tag{81}$$

we can observe that the ratio of the last term to the first term is

$$\frac{N^2H^2}{f^2L^2}\frac{fL^2}{\kappa_{h_I}}\frac{r}{Hf} \approx \frac{\sigma S}{E_h}E_v^{\frac{1}{2}} = \frac{\sigma S}{E_v^{\frac{1}{2}}}\frac{E_v}{E_h}. \tag{82}$$

So, as in the rotating cylinder case, when $\frac{\sigma S}{E_v^{\frac{1}{2}}} >> 1$, the interior velocity nearly satisfy the boundary condition.

2.2.4 Results

The results for this special case are shown in figure 7 and 8.

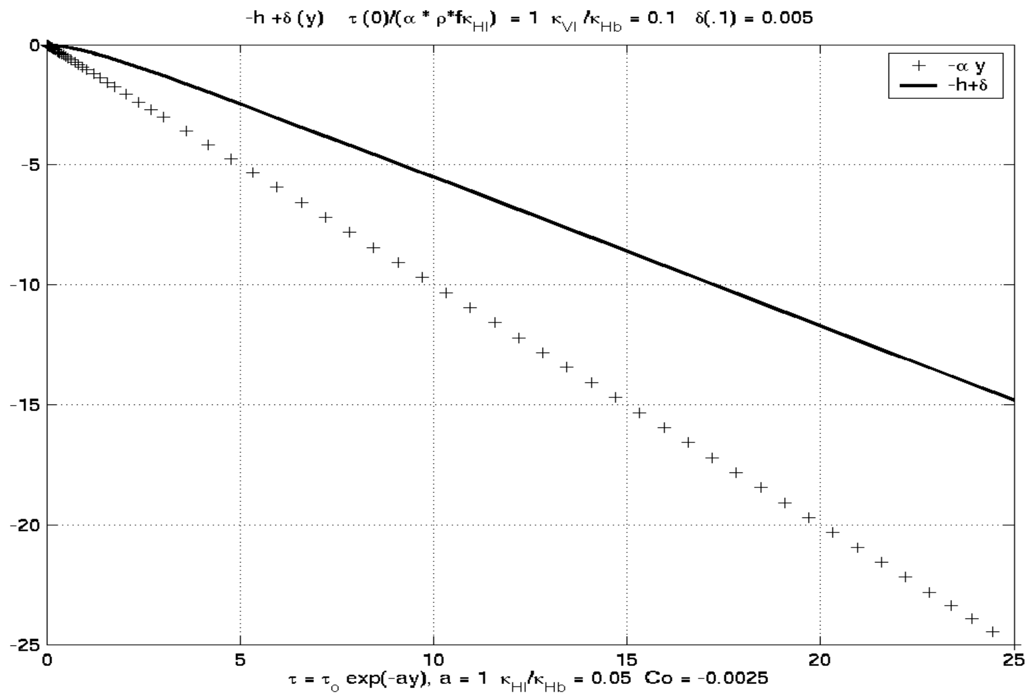

Figure 7: The boundary layer thickness with respect to the sloping bottom for $a = 1$, $\Sigma_v = 0.1$, $\Sigma_h = 0.05$. A starting value of δ of the depth at $y = y_0 = 0.01$ is chosen and C is -0.0025. $F = 1$ has been used.

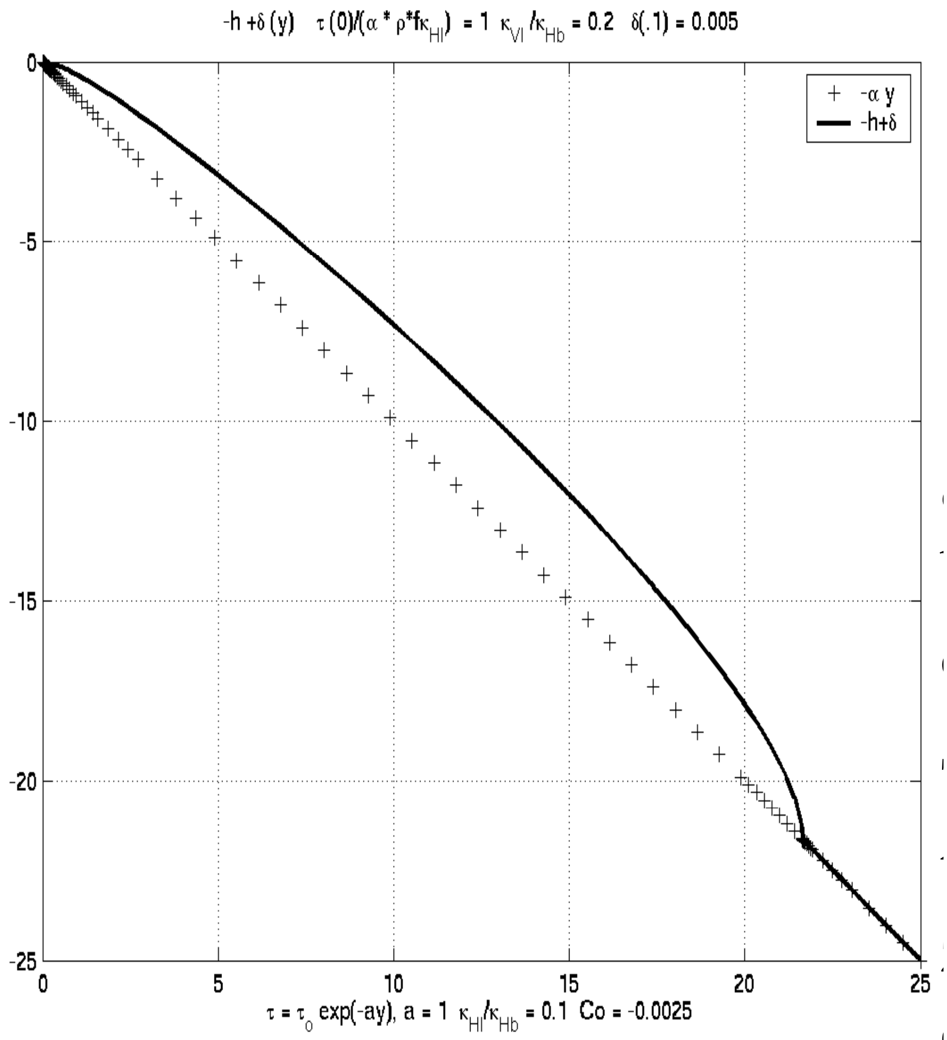

Figure 8: For larger coefficients in the interior, $\Sigma_v = 0.2$, $\Sigma_h = 0.1$, δ goes to zero well beyond the region of wind stress. The interior velocity then satisfies the zero velocity condition.

References

David C. Chapman and Steven J. Lentz. Adjustment of stratified flow over a sloping bottom*. *Journal of Physical Oceanography*, 27(2):340–356, 1997. URL http://dx.doi.org/10.1175%2F1520-0485%281997%29027%3C0340%3AAOSFOA%3E2.0.CO%3B2.

Parker MacCready and Peter B. Rhines. Slippery bottom boundary layers on a slope. *Journal of Physical Oceanography*, 23(1):5–22, 1993. URL http://dx.doi.org/10.1175%2F1520-0485%281993%29023%3C0005%3ASBBLOA%3E2.0.CO%3B2.

G. K. Vallis. *Atmospheric and Oceanic Fluid Dynamics: Fundamentals and Large-Scale Circulation*. Cambridge University Press, Cambridge, U.K., 2006.